Sex-Specific Effects of the β3-Adrenergic Receptor Agonist Mirabegron in a Murine Two-Hit Heart Failure Model with Preserved Ejection Fraction

Sara-Ève Thibodeau , Élisabeth Walsh-Wilkinson , Emylie-Ann Labbé , Jacques Couet *

Posted Date: 28 September 2025

doi: 10.20944/preprints202509.2326.v1

Keywords: beta3 adrenergic receptor; mirabegron; heart failure; brown fat; cardiac hypertrophy; HFpEF

Article

Sex-Specific Effects of the β3-Adrenergic Receptor Agonist Mirabegron in a Murine Two-Hit Heart Failure Model with Preserved Ejection Fraction

Sara-Ève Thibodeau [1,2,3], Élisabeth Walsh-Wilkinson [1,2,3], Emylie-Ann Labbé [1,2,3] and Jacques Couet [1,2,3,*]

[1] Département de Médecine, Faculté de Médecine, Université Laval, Québec City, QC G1V 0A6, Canada
[2] Groupe de Recherche sur les Valvulopathies, Centre de Recherche de l'Institut Universitaire de Cardiologie et de Pneumologie de Québec, Université Laval, Québec City, QC G1V 4G5, Canada
[3] Centre de recherche de l'Institut universitaire de cardiologie et de pneumologie de Québec, Université Laval, Québec City, QC, Canada
* Correspondence: Jacques.couet@med.ulaval.ca.: (J.C.)

Abstract

Background. In addition to its role in thermogenesis, activation of the brown adipose tissue (BAT) has been shown to produce factors (batokines) that can protect the cardiovascular system, particularly the heart, in pathological situations such as hypertension, atherosclerosis, and ischemia/reperfusion injury, BAT activation is mediated via the β3-adrenergic receptor (β3-AR), which is abundantly expressed in this tissue. In this study, we investigated whether using a specific β3-AR agonist, mirabegron, could slow the development of heart failure with preserved ejection fraction (HFpEF) in C57Bl6/J male and female mice after a metabolic-hypertensive stress (MHS). **Methods.** Eight-week-old mice of both sexes were divided into four groups. Control, mirabegron (Mira) (2 mg/kg/day), MHS (Angiotensin II [1.5mg/kg/day] + a high-fat diet) or MHS + mirabegron for 28 days. At the end of the protocol, all animals had an echocardiography exam, and the heart, lungs, BAT and liver were collected. **Results.** After four weeks of MHS, the indexed heart weight was significantly increased in all groups, but to a lesser extent in mice that received Mira. The expected left atrial enlargement following the HFpEF-inducing stress, MHS, was present in all groups, but was less in Mira male mice. Body growth was reduced in males receiving Mira. Echocardiography showed that males receiving Mira had smaller left ventricles (LV) and higher ejection fraction. Following the MHS, an expected increase in the expression of several marker genes associated with cardiac hypertrophy or fibrosis was observed in males, but not in females. Mirabegron treatment increased BAT volume in males but had a lesser effect in females. Uncoupled protein 1 (Ucp1) gene expression in the BAT was also in males but not in females. MHS alone also increased Ucp1 and β3-AR mRNA levels in BAT only in males. **Conclusion.** Male mouse hearts are more responsive to β3-AR activation by mirabegron, a specific agonist, than female hearts. This translates to a blunted hypertrophic response to the MHS and reduced LV expression of genes commonly increased in pathological cardiac conditions.

Keywords: beta3 adrenergic receptor; mirabegron; heart failure; brown fat; cardiac hypertrophy; HFpEF

1. Introduction

Heart failure with preserved ejection fraction (HFpEF) is a multifactorial syndrome usually resulting from various non-addressed risk factors, such as hypertension, obesity and diabetes, hypertension, kidney diseases, atrial fibrillation, tobacco, age, and the female sex (menopause) [1].

 doi:10.20944/preprints202509.2326.v1

HFpEF is associated with high morbidity and mortality (reaching up to 80% and 50%, respectively, within a 5-year after diagnosis) and represents more than 50% of HF-related hospitalizations [2].

Several preclinical models of HFpEF have been developed, notably the L-NAME (nitric oxide synthase inhibition) + high-fat diet (HFD) mouse model, introduced by Schiattarella et al. [3], which initiated the trend of combining "hits" to induce the syndrome in animals. [4–7] Most of these new models involve an approach targeting major HFpEF risk factors such as hypertension and metabolic alterations. [7] These animal models all display cardiac hypertrophy (CH), concentric left ventricle (LV) remodelling, diastolic dysfunction, myocardial fibrosis and preserved LV ejection fraction (EF). Pulmonary congestion, exercise intolerance, and elevated natriuretic and inflammatory markers are typically present. Some models were characterized in both sexes, as females often show a less severe phenotype.[7]

The HFpEF model in C57Bl/6J mice that we recently developed (the MHS model) is also based on the combination of hypertension (Angiotensin II [AngII] continuous infusion) and metabolic alterations induced by a high-fat diet (HFD) for 28 days. [8] This model is reproducible and induces the expected HFpEF features such as CH, LV concentric remodelling, LA enlargement and decreased exercise capacity in both male and female mice. This combination of stress induces HFpEF in older females, irrespective of their hormonal status (ovariectomized or not). [8,9] Old males (20 months), however, tend to evolve toward HFrEF. [9]

HFpEF has long been recognized as a multifaceted syndrome affecting multiple organs. It is estimated that around 80% of HFpEF patients are obese, suggesting that the adipose tissue may be a significant contributing factor in the development of this condition. Obesity is associated with a chronic inflammatory state that can exacerbate the severity of other HFpEF risk factors, such as aging, hypertension, kidney disease, and atrial fibrillation, among others.

We observed in the MHS model that the circulatory microRNA (miR) profile was strongly perturbed. The adipose tissue, along with the liver, is a significant source of miRs found in the circulatory system [10]. More recently, we reported that cold housing exacerbated the HFpEF phenotype in mice [11]. Thermoneutrality in mice is estimated to be around 29-32°C. At these temperatures, thermogenesis, which involves the activation of the brown adipose tissue (BAT), is at its minimum. Animals housed at 30°C had a less severe HFpEF phenotype compared to those at standard room temperature (22°C). Housing at 10°C resulted in mice exposed to the MHS in a loss of EF.

β3-adrenergic receptor (β3-AR) activation stimulates the production of factors by the BAT that are believed to protect the cardiovascular system in pathological situations, such as heart failure. [12,13]

Here, instead of using cold to induce BAT activation, we relied on a specific β3-adrenergic receptor (β3-AR) agonist, mirabegron (Mira). Mira has been shown to dampen cardiac remodelling in male mice treated with AngII [14,15]. Here, we demonstrate that Mira had sex-specific effects on the cardiac response to the MHS, with a greater benefit observed in male mice compared to females.

2. Materials and Methods

Animals

C57BL/6J male and female 7-week-old mice were purchased from the Jackson Laboratory (Bar Harbor, ME, USA). Mice were housed (3-4 mice/cage) on a 12-hour light-12-hour dark cycle with free access to food and water. The protocol was approved by the Université Laval's animal protection committee and followed the recommendations of the Canadian Council on Laboratory Animal Care (#2023-1249). This study was conducted in accordance with the ARRIVE guidelines. Mice were randomly assigned to the various experimental groups: controls, MHS, Mirabegron (Mira), and MHS + Mira. The experimental design is schematized in Figure 1A.

 doi:10.20944/preprints202509.2326.v1

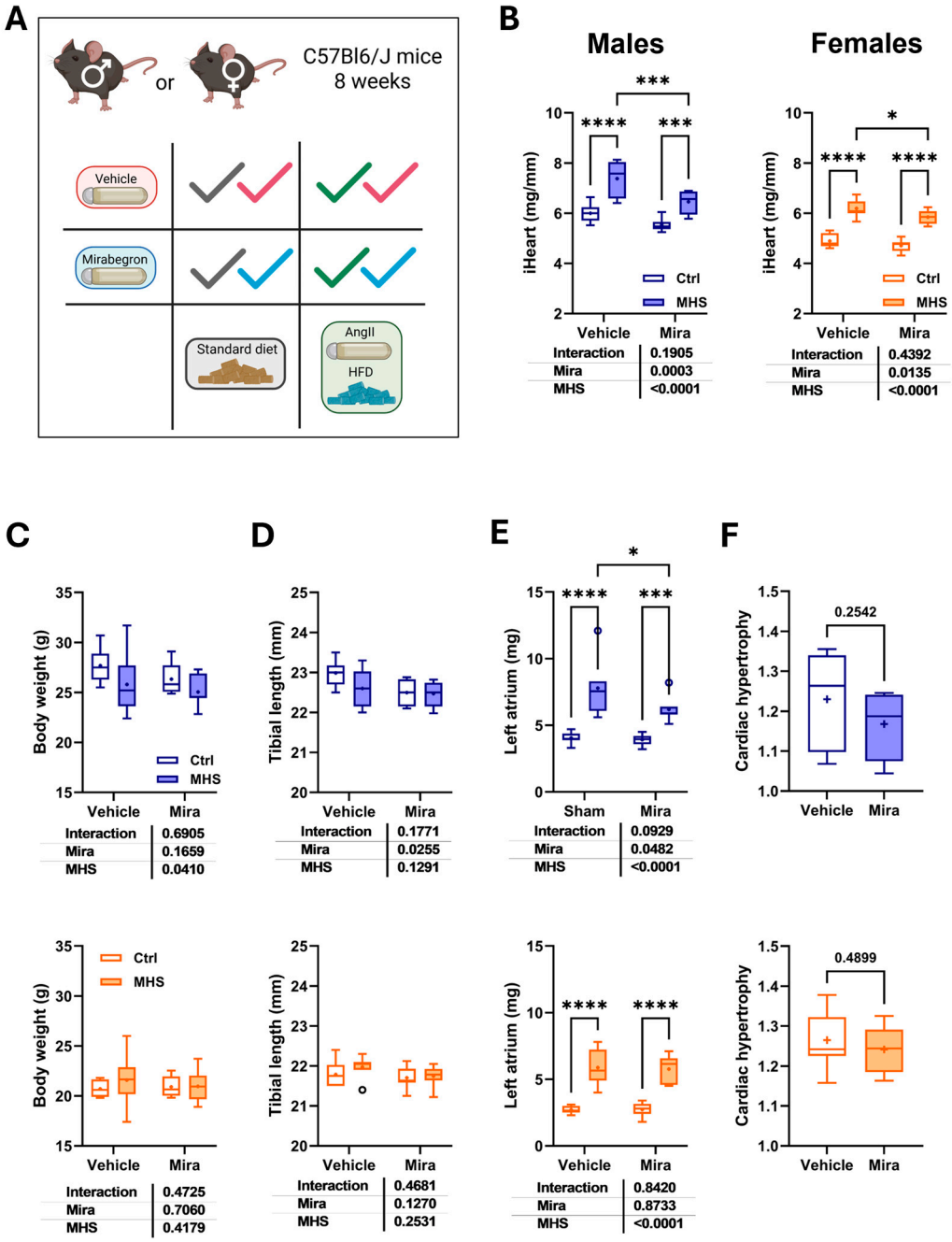

Figure 1. Effects of mirabegron on the mouse body and cardiac morphology in the presence of the MHS or not. A. Schematic representation of the experimental design (Created in BioRender. Couet, J. (2025) https://BioRender.com/wmcm34z). Eight-week-old C57BL/6J male and female mice were divided into four groups for 28 days: control mice on a standard diet and receiving the vehicle, MHS mice treated with the vehicle, control mice treated with mirabegron (Mira), and MHS mice receiving Mira. B. Indexed heart weight for tibial length (iHeart). Males: blue and left panel. Females: orange and right panel. C. Body weight. Males: blue and upper panel. Females: orange and the bottom panel. D. Tibial length E. Left atrial weight. F Cardiac hypertrophy. Ratio of the heart weight of MHS mice to the average heart weight of the corresponding control group. Results are expressed as mean ± standard error of the mean (SEM)—two-way ANOVA followed by Fisher's Least Significant Difference (LSD) test. The results of the two-way ANOVA are presented below the graph for each variable and the Interaction (MHS × Mira). *: $p<0.05$, **: $p<0.01$, ***: $p<0.001$ and ****: $p<0.0001$ between indicated groups (n=7-8 mice/group).

 doi:10.20944/preprints202509.2326.v1

Mice were randomly assigned to the various experimental groups (n = 7-8 per group). Experienced technicians monitored the mice's health and behaviour daily during the protocol, and the animals were weighed weekly. Three intact male mice died in the MHS group.

Metabolic and hypertensive stress (MHS). As described before, mice were implanted with an osmotic minipump (Alzet #1004) providing a continuous infusion of angiotensin II (AngII; 1,5mg/kg/day) (Sigma) for 28 days and fed with a high-fat diet (HFD: 60% calories; Research Diets Cat. #D12492). [8] Mirabegron (Toronto Research Chemicals, Toronto, Canada) treatment. Mice were implanted with an osmotic minipump (Alzet #1004) that provided a continuous infusion of mirabegron (dissolved in DMSO and PEG400 [Vehicle]; 2 mg/kg/day) (Sigma) for 28 days. Experienced technicians monitored the mice's health and behaviour daily during the protocol, and the animals were weighed weekly.

Echocardiography

Echocardiography was performed under isoflurane anesthesia as described previously (8, 16).

RNA Isolation and Quantitative Real-Time Polymerase Chain Reaction

As described previously, total RNA was extracted from LV tissue (8). Quantitative RT-PCR was used to quantify LV gene expression in at least six animals per group. Cyclophilin A (*Ppia*) served as the control "housekeeping" gene for studying cardiac genes, while RPL13 was used for studying brown fat genes. The primers used are listed in Table 1.

Table 1. Sequences of primers used in this study.

Symbol	Description	Forward sequence Reverse sequence
Col1a1	Collagen Type I Alpha 1 Chain	5′-CAT TGT GTA TGC AGC TGA CTT C-3′ 5′CGC AAA CAC TCT ACA TGT CTA GG-3′
Col3a1	Collagen Type III Alpha 1 Chain	5′-TCT CTA GAC TCA TAG GAC TGA CC-3′ 5′ TTC TTC TCA CCC TTC TTC ATC C-3′
Nppa	Natriuretic Peptide B	5′-CTC CTT GGC TGT TAT CTT CGG-3′ 5′-GGG TAG GAT TGA CAG GAT TGG-3′
Nppb	Natriuretic Peptide A	5′-AGG TGA CAC ATA TCT CAA GCT G-3′ 5′-CTT CCT ACA ACA TCA GTG C-3′
Ppia	Cyclophilin A	5′-TTC ACC TTC CCA AAG ACC AC-3′ 5′-CAA ACA CAA ACG GTT CCC AG-3′
Postn	Periostin	5′-GCT TTC GAG AAA CTG CCA CG-3′ 5′-ATG GTC TCA AAC ACG GCT CC-3′
Thbs4	Thrombospondin 4	5′-GAT ACT GAC GGG GAT GGG AG-3′ 5′-CGT CAC TGT CTT GGT TGG TG-3′
Ucp1	Uncoupled protein 1	5′-GCT TCT ACG ACT CAG TCC AA-3′ 5′-CTC TGG GCT TGC ATT CTG AC-3′
Adrb3	Adrenoceptor Beta 3	5′-AGG AAG CTT GCT TGA TCC-3′ 5′-AGG AAG CTT GCT TGA TCC-3′
Rpl13	Ribosomal Protein L13	5′-CGG CTG AAG CCT ACC AGA AA-3′ 5′-GGA GTC CGT TGG TCT TGA GG-3′

Myocardial Fibrosis Evaluation

Myocardial samples were fixed, sliced in serial sections (10μm thick), and stained with Picrosirius Red to assess the percentage of interstitial fibrosis. The formula used to calculate the percentage of interstitial fibrosis was: ((% Fibrosis) / (% Fibrosis + % Tissue)) × 100 [17]. Perivascular fibrosis was not included in the estimation of interstitial fibrosis.

Cardiomyocyte Cross-Sectional Area

The cardiomyocyte cross-sectional area (CSA) was visualized with immunofluorescent wheat germ agglutinin-FITC (Sigma) staining as previously described [17].

BAT Histology

 doi:10.20944/preprints202509.2326.v1

BAT samples were preserved in a 4% paraformaldehyde solution for 24 hours and transferred to 70% ethanol. The specimens were paraffin-embedded, cut into 4-µm sections and stained with hematoxylin and eosin.

Statistical Analysis

All data are expressed as mean ± standard error of the mean (SEM). Outliers were removed using the ROUT test with a Q of 1% with Prism. Intergroup comparisons were conducted using the Student's T-test using GraphPad Prism 10.6 (GraphPad Software Inc., La Jolla, CA, USA). Comparisons among more than two groups were analyzed using a two-way ANOVA followed by Fisher's Least Significant Difference (LSD) test. $P<0.05$ was considered statistically significant.

3. Results

3.1. Mirabegron, a β3-Adrenergic Receptor Agonist, Has Sex-Specific Effects on Body and Cardiac Growth in Young C57BL/6 Mice

As illustrated in Figure 1A, C57Bl6/J male and female mice received AngII and the high-fat diet (HFD) for four weeks (MHS) alongside or not with mirabegron for 28 days. Control mice receiving the vehicle or mirabegron (Mira) alone were studied in parallel.

Indexed heart weight (for tibial length) was lowered in animals treated with mirabegron (Figure 1B). MHS mice receiving Mira also had a smaller heart, although the stress caused cardiac hypertrophy. Body weight remained unchanged in mice receiving Mira, but body growth (as measured by tibial length) was reduced in males, not in females (Figures 1C and 1D).

The MHS has been shown to lead to left atrial (LA) enlargement [8]. We observed this in mice of both sexes. However, LA were smaller in MHS males receiving Mira. This was not the case for females. (Figure 1E). Overall, we did not observe differences in the levels of cardiac hypertrophy (compared to the respective control groups) in mice treated with Mira (Figure 1F) compared to those not treated.

Figure 2 shows cardiac morphological and functional changes induced by the MHS in mice treated or not with Mira. As illustrated in Figures 2A-C, the MHS, as expected, induced LV concentric remodelling, characterized by increased left ventricle (LV) wall thickness and a decreased LV diastolic diameter, resulting in an increased LV relative wall thickness or RWT (LV wall thickness/EDD). In mice treated with Mira, LV walls were thicker in males, EDD was smaller, and RWT was thus increased compared to male animals not receiving Mira. In females, the effects of Mira were not present, except for a slight reduction of EDD.

Table 2 summarizes additional echo measurements in our mice. Diastolic interventricular septum thickness (IVSd) and end-systolic diameter (ESD) were reduced in MHS+Mira males compared to the MHS-only group. This was not the case for females. Using bidimensional echocardiography LV imaging, we calculated volumes and ejection fraction using Simpson's method. As illustrated in Figures 2D and 2E, end-diastolic (EDV) and end-systolic (ESV) LV volumes were reduced in male animals treated with Mira but not in females. Interestingly, this resulted in a higher ejection fraction (EF) in males. Cardiac output (CO) remained stable in all groups (Table 2).

 doi:10.20944/preprints202509.2326.v1

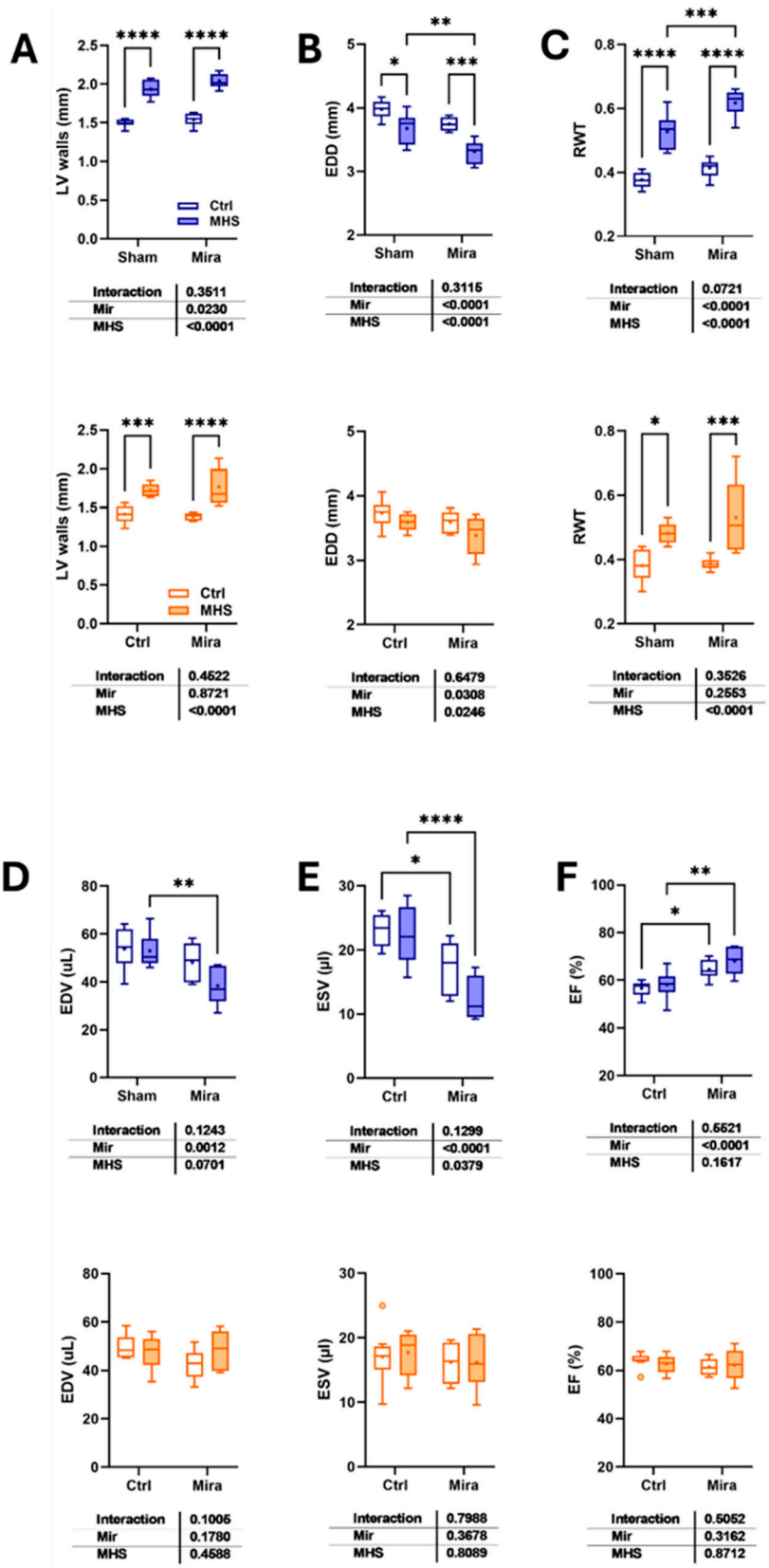

Figure 2. Mirabegron (Mir) reduces left ventricular volumes and increases EF in males but not females. A. Diastolic LV wall thickness (posterior + septal). Males: blue and upper panel. Females: orange and the bottom panel. B. End-diastolic LV diameter (EDD). C. Relative wall thickness (RWT; LV walls/EDD). D. End-diastolic volume (EDV). E. End-systolic volume (ESV) and F. LV ejection fraction (EF; (EDV-ESV)/EDV * 100). Results are expressed as mean ± standard error of the mean (SEM)—two-way ANOVA followed by Fisher's LSD test. The results of the two-way ANOVA are presented below the graph for each variable and the interaction (MHS × Mira). *: p<0.05, **: p<0.01, ***: p<0.001 and ****: p<0.0001 between indicated groups (n=7-8 mice/group).

 doi:10.20944/preprints202509.2326.v1

Table 2. Echo data in male and female mice after MHS and/or Mirabegron (Mira). Controls (C). Vehicle (Veh). Echo exams as described in the Methods section. PWd: diastolic posterior wall thickness, IVSd: diastolic interventricular septum, ESD: end-systolic LV diameter, LVM: LV mass, SV: stroke volume, HR: heart rate, CO: cardiac output. Results are expressed as the mean ± standard error of the mean (SEM). P values were calculated using Fisher's LSD test after a two-way ANOVA. a: p<0.05 vs respective control group, b: p<0.01, c: p<0.001 and d: p<0.0001. e: p<0.05 vs respective Veh group, f: p<0.01, g: p<0.001 and h: p<0.0001.

Males							
Parameters	**Ctrl/Veh(n=8)**	**MHS/Veh(n=8)**	**Ctrl/Mira(n=8)**	**MHS/Mira (n=7)**	**MHS**	**Mira**	**MHS X M**
PWd, mm	0.79±0.016	1.03±0.027d	0.75±0.014	1.05±0.021d	<0.0001	0.52	0.087
IVSd, mm	0.75±0.013	0.91±0.023d	0.75±0.013	0.99±0.020d,g	<0.0001	0.032	0.028
ESD, mm	2.79±0.075	2.77±0.098	2.40±0.085f	2.01±0.071b,h	<0.0001	0.026	0.034
LVM, mg	106±1.8	134±5.1d	100±2.5	123±5.2c	<0.0001	0.046	0.57
SV, mm	31±2.2	31±1.5	31±1.7	26±1.3	0.22	0.27	0.22
HR, bpm	498±10.4	513±17.0	518±14.0	561±11.7a,e	0.044	0.021	0.31
CO, ml/min	15.2±1.07	15.8±1.05	15.9±0.60	14.6±1.22	0.71	0.81	0.37
Females							
Parameters	**Ctrl/Veh (n=8)**	**MHS/Veh (n=8)**	**Ctrl/Mira(n=8)**	**MHS/Mira (n=8)**	**MHS**	**Mira**	**MHS X M**
PWd, mm	0.71±0.024	0.88±0.024b	0.71±0.011	0.96±0.056c	<0.0001	0.23	0.27
IVSd, mm	0.70±0.020	0.84±0.015d	0.67±0.010	0.81±0.031d	<0.0001	0.15	0.90
ESD, mm	2.52±0.105	2.33±0.061	2.34±0.096	2.20±0.076	0.0680	0.088	0.78
LVM, mg	88±1.7	109±3.2d	81±2.9	103±4.0d	<0.0001	0.044	0.83
SV, mm	31±0.7	30±1.5	25±0.7g	26±1.3e	0.62	0.0022	0.26
HR, bpm	516±11.2	528±6.0	514±15.0	538±17.6	0.19	0.74	0.67
CO, ml/min	15.4±0.85	15.6±0.84	13.1±0.43e	14.0±0.46	0.40	0.0061	0.64

We measured diastolic function parameters using echocardiography (Table 3). We had observed in previous studies that four weeks of MHS was not sufficient to induce pulmonary congestion, but prolonging the stress up to eight weeks increased lung water content (Figure 3A). Here, we observed that Mira treatment increased lung water content in both control and MHS mice. This water content was not higher in MHS mice, however. Liver weight was increased in males by Mira but not in females (Figure 3B). The MHS reduced liver weight in all female groups, but only in males treated with Mira.

 doi:10.20944/preprints202509.2326.v1

Table 3. Echo diastolic parameters in male and female mice after MHS and/or Mirabegron (Mira). Controls (C). Vehicle (Veh). Echo exams as described in the Methods section. E wave velocity, A wave velocity, E wave slope, Isovolumetric relaxation time (IVRT), E' wave velocity, A' wave velocity and LA diameter. Results are expressed as the mean ± standard error of the mean (SEM). P values were calculated using Fisher's LSD test after a two-way ANOVA. a: p<0.05 vs respective control group, b: p<0.01, c: p<0.001 and d: p<0.0001. e: p<0.05 vs respective Veh group, f: p<0.01, g: p<0.001 and h: p<0.0001.

Males							
Parameters	**Ctrl/Veh(n=8)**	**MHS/Veh(n=8)**	**Ctrl/Mira(n=8)**	**MHS/Mira(n=7)**	**MHS**	**Mira**	**MHS X M**
E, mm/s	659±14.8	537±21.0c	653±23.7	533±21.2c	<0.0001	0.81	0.97
A, mm/s	431±16.5	388±21.1	391±13.5	405±19.9	0.43	0.49	0.12
E slope	-39160±2804	-33681±1799	-37444±1566	-33247±2466	0.037	0.63	0.77
IVRT, ms	16.8±0.53	16.0±0.35	15.7±0.49	15.3±0.47	0.24	0.48	0.80
E', mm/s	29.4±0.99	24.0±1.90b	30.0±0.77	22.8±0.75c	<0.0001	0.82	0.50
A', mm/s	17.8±0.81	16.5±1.29	14.9±0.44e	14.8±0.96	0.46	0.021	0.55
E/A	1.5±0.04	1.4±0.03a	1.7±0.05e	1.3±0.05d	<0.0001	0.40	0.020
E/E'	20.8±1.17	21.1±0.90	21.9±0.94	23.7±1.20	0.32	0.96	0.58
LA diam, mm	2.34±0.049	2.46±0.081	2.18±0.041	2.42±0.067b	0.0058	0.11	0.32
Females							
Parameters	**Ctrl/Veh(n=8)**	**MHS/Veh(n=8)**	**Ctrl/Mira(n=8)**	**MHS/Mira(n=8)**	**MHS**	**Mira**	**MHS X M**
E, mm/s	560±23.9	604±28.9	532±11.3	650±45.2b	0.012	0.76	0.22
A, mm/s	374±11.8	398±21.8	315±7.2	302±22.3	0.74	<0.0001	0.29
E slope	-38869±1323	-35653±2291	-36251±1234	-39024±4731	0.89	0.94	0.29
IVRT, ms	15.1±0.29	16.1±0.57	15.9±0.47	16.0±0.43	0.44	0.29	0.32
E', mm/s	30.5±0.29	24.1±1.10c	29.6±0.67	26.5±1.20a	<0.0001	0.14	0.33
A', mm/s	18.5±0.78	17.8±0.67	16.0±0.43e	13.0±1.31a,f	0.029	0.0003	0.31
E/A	1.6±0.04	1.5±0.07	1.7±0.06	2.2±0.20b,g	0.0004	0.018	0.031
E/E'	18.6±0.71	23.1±1.23b	18.1±0.65	24.6±1.15c	<0.0001	0.20	0.43
LA diam, mm	2.13±0.0027	2.30±0.053a	2.13±0.055	2.38±0.088b	0.0017	0.48	0.49

We then measured the mRNA levels of six genes associated with pathological hypertrophy. Gene expression of the atrial natriuretic peptide (*Nppa*) was, as expected, increased in MHS mice not receiving Mira. In females treated with Mira, MHS caused a similar increase in *Nppa,* but this increase was almost completely obliterated in males (Figure 3C). Brain natriuretic peptide (*Nppb)* gene expression was increased by the MHS in both male and female mice, but at a significantly lower level in females (Figure 3D). We had observed in the past that collagens (*Col1a* and *Col3a*) mRNA levels were minimally or not modulated in females after 28 days of MHS, although myocardial fibrosis content was increased [8,9,17]. We confirmed this previous observation, and Mira had no additional effects. In males, mRNA levels for these two genes were increased by MHS; however, Mira completely blocked this effect (Figures 3E and 3F). We also measured genes associated with myocardial fibroblast activation, specifically periostin (*Postn*) and Thrombospondin 4 (*Thbs4*). In animals receiving the vehicle, both gene mRNA levels were increased. This was blunted in males receiving Mira, but not in females. (Figures 3G and 3H)

 doi:10.20944/preprints202509.2326.v1

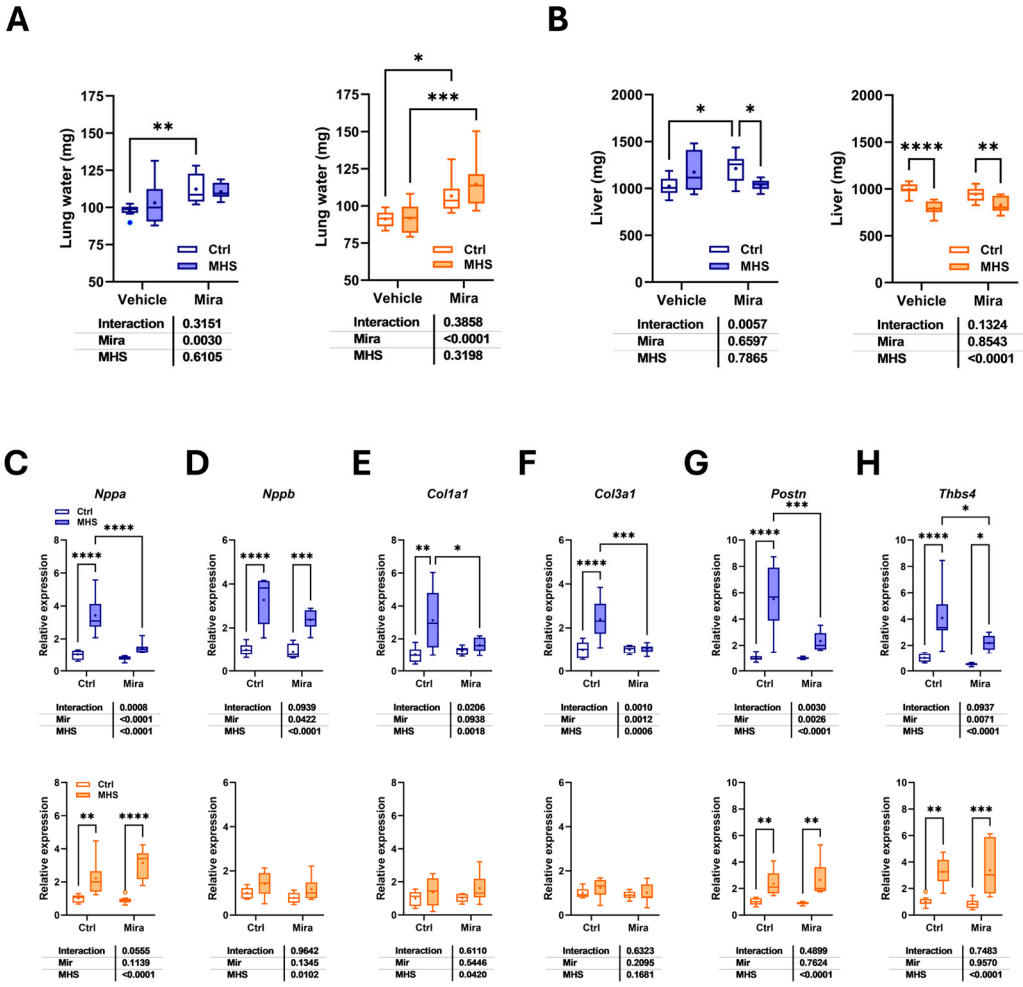

Figure 3. Mirabegron sex-specific effects on lungs, liver and on pathological LV hypertrophy gene expression. A. Lung water content (Wet lungs weight – Dry lungs weight). B. Liver weight. Males: blue and left panel. Females: orange and right panel. LV gene expression in control and MHS treated or not with Mira. Males: blue and upper panel. Females: orange and the bottom panel. C. Atril natriuretic peptide (*Nppa*). D. Brain natriuretic peptide (*Nppb*), E. Collagen 1 alpha (*Col1a1*), F. Collagen 3 alpha (*Col3a1*), G. Periostin (*Postn*). H. Thrombospondin 4 (*Thbs4*). Results are expressed as mean ± SEM, with two-way ANOVA followed by Fisher's LSD test. The results of the two-way ANOVA are presented below the graph for each variable and the interaction. *: p<0.05, **: p<0.01, ***: p<0.001 and ****: p<0.0001 between indicated groups (n=7-8 mice/group).

We then studied the scapular brown adipose tissue (BAT) depot of our mice. As illustrated in Figure 4A, Mira treatment led to an increase in the weight of BAT in control mice. This increase was more elevated in males than in females. Interestingly, the MHS partially reversed the effects of Mira in BAT. This can be visualized in Figure 4B, which shows representative pictures of the BAT depot from control Mira-treated female mice (top) and after MHS (bottom). The MHS BAT was also darker. This can be attributed to the lower fat content in brown adipocytes (Figure 4C) and smaller cell size, as illustrated in Figure 4D. To estimate the adipocyte size, we counted the number of nuclei in a microscope field. Except for vehicle-treated MHS males, all MHS groups had more nuclei and thus smaller brown adipocyte cell size.

Activation of the β3-adrenergic receptor (β3-AR) by Mira is expected to lead to an increase in thermogenesis and the expression of the mitochondrial uncoupling protein 1 (*Ucp1*) gene. As illustrated in Figure 4E, Mira treatment resulted in the expected rise in *Ucp1* mRNA levels in the BAT (Figure 4E). We also measured the β3-AR gene expression levels (*Adrb3*) in the BAT. Mira treatment

 doi:10.20944/preprints202509.2326.v1

did not affect these levels in control animals and MHS females. In MHS males, *Adrb3* gene expression was increased over control groups irrespective of Mira treatment (Figure 4F).

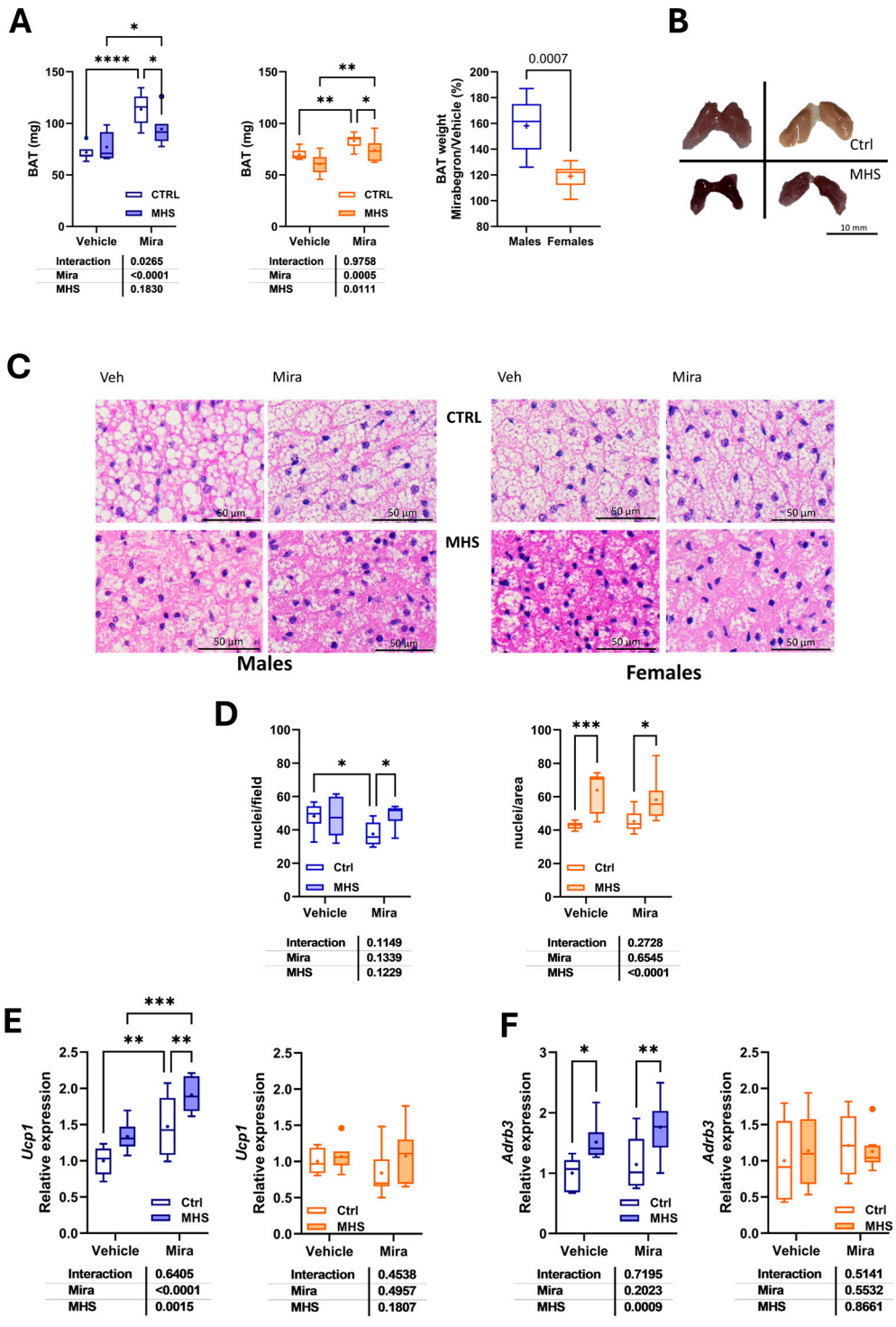

Figure 4. Effects of MHS and Mira on brown fat. A. Brown adipose tissue (BAT) scapular depot weight. Right panel: Increase in BAT weight in control mice treated with Mira. Males: blue and left panel. Females: orange and right panel. B. Representative pictures of the BAT depot in two female Mira-treated control mice (top) and two MHS mice. Scale bar: 10 mm. C. Hematoxylin/eosin-stained BAT sections from a mouse of each group. Scale bar: 50µm. D. Number of nuclei per microscope field. E. *Ucp1* mRNA levels in the BAT. F. *Adrb3* gene expression. Results are expressed as mean ± SEM. The results of the two-way ANOVA are presented below the graph for

 doi:10.20944/preprints202509.2326.v1

each variable and the interaction (MHS × Mira). *: p<0.05, **: p<0.01, ***: p<0.001 and ****: p<0.0001 between indicated groups (n=7-8 mice/group).

3.2. Mirabegron Effects on Cardiomyocyte and Extracellular Matrix Remodelling After MHS

The C57BL/6J mouse heart does not express the β3-adrenergic receptor gene. From the previously published LV bulk RNASeq data [8; GEO Accession Number: GSE240171], we illustrated in Figure 5A the LV gene expression of the β1, β2, and β3-AR genes. The normalized counts of each gene for control and MHS mice (three males and three females for each group) show that the β3-AR gene expression levels (*Adrb3*) in the LV are undetectable compared to the other two genes encoding these receptors. Interestingly, the levels of the β1-AR gene (*Adrb1*) were lower in MHS animals, but those of the β2 form (*Adrb2*) remained stable.

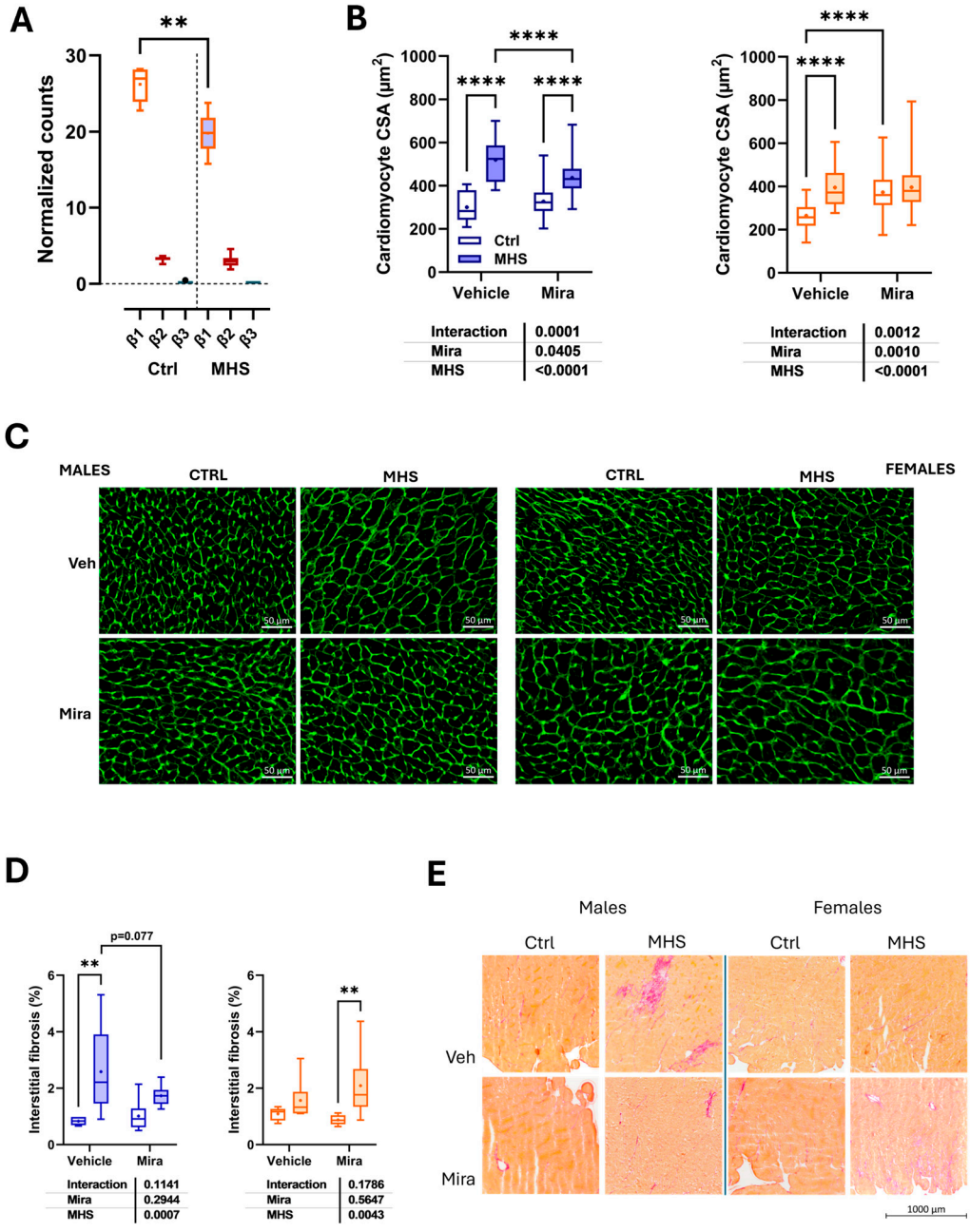

Figure 5. Beta-adrenergic receptor gene expression in the heart and myocardial morphological changes related to mirabegron treatment. A. Beta-adrenergic receptor subtypes mRNA levels in control and MHS mice. Using bulk RNA sequencing data from the LV of young control and MHS mice (three males and three females/group;

 doi:10.20944/preprints202509.2326.v1

GEO accession number: GSE240171), we extracted the normalized counts of the three adrenergic receptors (*Adrb1* or β1, *Adrb2* or β2 and *Adrb3* or β3) of control and MHS mice. B. Cardiomyocyte cross-sectional area. C. Representative images of WGA-FITC staining from LV sections of the various indicated groups. D. Myocardial interstitial fibrosis. E. Representative images of picrosirius red staining of male and female heart sections. Results are expressed as mean ± SEM. The results of the two-way ANOVA are presented below the graph for each variable and the interaction (MHS × Mira). *: $p<0.05$, **: $p<0.01$, ***: $p<0.001$ and ****: $p<0.0001$ between indicated groups (n=7-8 mice/group).

Cardiomyocyte size was estimated on LV sections stained with fluorescent wheat germ agglutinin (WGA). The MHS increased cardiomyocyte cross-sectional area (CSA) as expected in males treated with or without Mira. The CSA was smaller in males receiving Mira. In females, treatment with Mira increased the cardiomyocyte in control females, and the MHS did not lead to a further rise in this parameter (Figures 5B and 5C).

The MHS led to increased myocardial fibrotic content in males and females (Figures 5D and 5E). This rise in fibrosis tended to be reduced in males treated with Mira ($p = 0.077$).

4. Discussion

The adipose tissue is now regarded as an endocrine organ that secretes many factors, part of a complex network of interorgan crosstalk [18,19]. If this is largely recognized for the white adipose tissue, this is becoming increasingly accepted that BAT actively participates in this crosstalk. The BAT has long been regarded mainly as a thermogenic tissue, but its secretory activity is now recognized. "Batokines" are molecules secreted by the BAT, and several pieces of evidence support that they provide several benefits to other systems, including the cardiovascular system. [20,21]

In this study, we aimed to activate the BAT using a selective β3-AR agonist, mirabegron and investigate if it would benefit the heart in a murine HFpEF model. For several parameters measured, this was the case, but mainly in males. Male mice receiving Mira had after MHS, reduced body weight, shorter tibial length, lower indexed heart weight, and less atrial enlargement. Females treated with Mira maintained their body weight, and tibial length remained unchanged. Left atrial enlargement was similar after MHS in mice treated with Mira compared to females not receiving Mira. Still, females treated with Mira had smaller hearts.

When analyzed by echocardiography, control Mira-treated male hearts had thicker LV walls, smaller LV chamber and increased EF. Females did not show this response to Mira. However, stroke volume and cardiac output were lowered by Mira treatment in females, but not in males. Mira did not modulate the echo diastolic parameters in males, but in females, the A and A' waves were lower, suggesting the atrial contraction may have been affected.

We observed that mice express almost undetectable LV levels of the *Adrb3* gene in both control and MHS animals. As expected, the β1-AR and β2-AR were the primary forms expressed in the left ventricle of the mice. The expression of the β1-AR form was reduced in HFpEF animals, suggesting downregulation that may be due to an excess of circulating catecholamines. The mRNA levels of the β3-AR mRNA were too low for detection in all mice. This indicates that mirabegron effects were most likely the result of its action on extra-cardiac tissues, notably the BAT, but not only. The β3-AR is also present in white adipose tissue (WAT) depots, and its activation can lead to beiging [22,23]. In the WAT, the β3-AR is present in beige or "brite" adipocytes (brown adipocytes located in the WAT), and its activation results in the activation of thermogenesis in the WAT [24]. This beiging phenomenon likely changes the amount or nature of factors usually released by the WAT. It is thus expected that Mira may have modulated factors secreted by the WAT in our mice, which in turn could have affected the heart.

Evidence suggests that the β3-adrenergic receptor (β3-AR) is upregulated in the failing heart in both human and animal models. [25–27] How do we reconcile our observations with these previous reports? Firstly, in the normal heart, β3-AR is low and possibly, the nature of the pathological stress

 doi:10.20944/preprints202509.2326.v1

may influence its up-regulation. Second, in previous studies, upregulation was observed in end-stage ischemic or dilated cardiomyopathies, whereas here, it is observed in a model of HFpEF.

In humans, activation of the β3-adrenergic receptor is associated with endothelial relaxation and reduced myocardial contractility. [28] The cardiac levels of β3-AR have been shown to rise in patients with heart failure [25,26]. Again, the cardiac β3-AR levels are one to two orders of magnitude less than the β1-AR or the β2-AR. Overexpressing the human β3-AR in the mouse heart has been shown to protect it from pathological hypertrophy and abnormal fibrosis in response to neurohormonal stimulation [29]. Cardiac β3-AR expression also protects against ischemia-reperfusion injury in mice [30]. These benefits were shown to be mediated via the coupling of this receptor to nitric oxide and via antioxidant protective effects.

Mirabegron is primarily used in the treatment of overactive bladder syndrome [31]. Still, two clinical trials have been conducted in patients with heart failure to explore the potential benefits of β3-AR activation. The results of these trials (one conducted in NYHA functional class III and IV patients and the other in NYHA I and II patients) were neutral [32–34]. Another study in patients with combined pre- and post-capillary pulmonary hypertension associated with symptomatic HF also resulted in neutral outcomes [35].

The β3-AR is highly expressed in the BAT, and the use of specific agonists, such as mirabegron, has often been employed to stimulate this fat depot in rodents [36–38]. As mentioned, it is challenging to attribute the effects of Mira solely to factors generated by the BAT. One way to show this would be to remove or inactivate the BAT.

In a rat model of metabolic syndrome (Dahl-Salt/obese rats), they observed that salt-loading hypertension was associated with whitening of the BAT and that its surgical removal would attenuate the exacerbation of LV diastolic dysfunction, inflammation, and fibrosis. *Ucp1* gene expression was reduced in the BAT of rats with metabolic syndrome, suggesting that normal BAT function is crucial for the cardiac response to pathological stress. [39]

In one of these studies, researchers induced pressure overload in mice by using abdominal aortic constriction and then kept them in a cold environment. Physical removal of interscapular BAT during cold exposure decreased thyroid hormone, T3, synthesis and mitigated pathological cardiac remodelling. However, mice harbouring a UCP1 KO and eliminating thermogenesis but preserving BAT integrity, they observed increased T3 synthesis and exacerbated pathological remodelling. This study suggests that there are differences between BAT ablation and inactivation in their roles in controlling thyroid hormone synthesis.[40]

BAT surgical removal was shown to block the benefits from exercise in a myocardial ischemic-reperfusion model in the mouse. They demonstrated that the BAT secretes small extracellular vesicles and that their miR content regulates cardiomyocyte survival and participates in exercise cardioprotection. [41]

Taken together, these studies show the interaction between the BAT and the heart. Others tried to identify factors other than miRs that could mediate the protective function of the BAT on the heart. The fibroblast growth factor 21 has been proposed as one of these factors.

A link between activation of the α2-AR/FGF21 axis in the BAT and the heart has been unveiled in DOCA-salt-treated mice (a hypertension model). Ablation of the α2-AR or of FGF21 in the BAT was shown to exacerbate the cardiac pathological phenotype, suggesting that the BAT was responsible for the production of cardioprotective factors such as FGF21. [42]

Another study investigating the effects of a α2-AR agonist (dexmedetomidine; DEX) in a mouse myocardial ischemia/reperfusion injury model also identified FGF21 as a cardioprotective factor. DEX increased circulating FGF21 levels, but BAT ablation countered the benefits of DEX treatment, suggesting that the FGF21 rise in concentration originated mainly from the BAT.[43]

In addition to FGF21, other batokines were shown to produce cardioprotective effects [44]. The batokine 12,13-dihydroxy-9Zoctadecenoic acid (12,13-diHOME) has been shown to improve cardiac hemodynamics by increasing cardiomyocyte contraction, relaxation, and mitochondrial respiration.

 doi:10.20944/preprints202509.2326.v1

Treatment with 12,13-diHOME blocks the effects of a high-fat diet on cardiac function and remodelling. [44]

The benefits of BAT function in cardiac pathological states have also been demonstrated using BAT implantation in the abdominal cavity of mice with LV pressure overload induced by transverse aortic constriction, or TAC. BAT implantation reduced the loss of EF in TAC mice. In a mouse model of aortic dissection/aneurysm, up-regulation of β3-AR in the perivascular adipose tissue. Activation of β3-AR by Mira significantly prevented AngII-induced AD/AA formation in mice. [45]

In our study, Mira treatment led to cardiac sex differences in both control and MHS mice. Assuming that Mira effects were mediated mainly via BAT activation of the β3-AR and secretion of batokines. The response of the heart to these batokines is thus sex-specific, suggesting that the nature or amount of these BAT factors differ between males and females. Our study was not designed to answer this question, and the paucity of studies on BAT physiology that investigated sex differences in mice leaves us with limited material to hypothesize about the reasons for these differences.

A recent study showed that activation of the BAT accelerated cardiac metabolic remodelling and reduced hypertrophic and fibrotic responses to pressure overload from TAC. [46] Interestingly, when animals were housed in a cold environment (16°C) to stimulate UCP1-dependent thermogenesis, this effect was not observed uniformly for males and females. At 16°C, females did not increase their UCP1 levels compared to room temperature (23°C). UCP1 levels were more elevated in females at 23°C than in males, suggesting that the cold stress from being housed at 23°C activated the BAT more in females.

We recently reported the effects of different housing temperatures on the HFpEF phenotype of MHS mice. [11] We did not observe significant sex differences in *Ucp1* gene expression between male and female animals. Housing at room temperature and in a cold environment (10°C in our case) was associated with a similar rise in *Ucp1* expression in both sexes. Unlike the study above, the MHS increased BAT *Ucp1* gene expression; however, this is likely linked to the effects of Angiotensin II on the BAT via the type 2 Ang II receptor.

We used AngII in the MHS model to induce hypertension and as a direct cardiac hypertrophic factor. As such, the MHS induces browning of the BAT in mice, accompanied by elevated *Ucp1* gene expression and decreased adipocyte size, suggesting the activation of this fat depot [11]. Although the high-fat diet in MHS is a known factor that induces obesity, its use in conjunction with AngII results in no body weight gain. [8, 9, 11, 17. The HFD without AngII for four weeks increased body weight in mice compared to a standard diet; however, AngII had the opposite effect in males. [8] Combining the two results in similar body weights in mice after four weeks, as per the MHS. The control of adiposity by angiotensin II is mediated by the Angiotensin II receptor type 2 (AT2R). AT2R KO results in increased obesity in mice fed an HFD, and its activation with a specific agonist (C21) blunts weight gain [47–49]. C21 can also lead to BAT activation (upregulation of *Ucp1*) and the browning of WAT in mice [49]. In the MHS model, the effects of AngII on the BAT seem to have overruled those of the high-fat diet.

Mirabegron is usually associated with a loss of body weight since activation of BAT thermogenesis reroutes energy consumption. [50] We observe this in males but not in females, who tend to maintain their body weight more consistently. Mira slowed body growth only in males. Interscapular BAT depot size was also increased more in males than in females.

5. Study Limitations

This study used a two-hit model to induce HFpEF that resembles human HFpEF. It is still not representative of the entire spectrum of HFpEF patients.

Mirabegron treatment was initiated simultaneously with the MHS, potentially slowing or preventing the development of HFpEF. This experimental design is not ideally suited to test the therapeutic potential of β3-AR activation in the context of an established heart disease.

 doi:10.20944/preprints202509.2326.v1

The translation of our results into human terms is challenging. Still, they emphasize that activation of the BAT is an interesting avenue worth pursuing in the future and that studying animals of both sexes can provide essential insights.

Several parameters were not measured in this study, including BP, animal metabolic activity, or daily activity, which may have affected our results.

6. Conclusions

Our results indicate that β3-AR activation via the specific agonist can benefit mice with HFpEF. These benefits seem to target more male animals, and the reasons for this need further research efforts to be uncovered.

Author Contributions: Conceptualization, S.-E. T., É.W.-W, and J.C.; methodology, S.-E. T., É.W.-W. et J.C.; validation, S.-E. T., É.W.-W. and J.C.; formal analysis, S.-E. T., É.W.-W. and J.C.; investigation, S.-E. T., É.W.-W., E.-A.L.; data curation, S.-E. T., É.W.-W., and J.C.; writing—original draft preparation, S.-E. T., and J.C.; writing—review and editing, J.C.; supervision, É.W.-W. and J.C.; project administration, J.C.; funding acquisition, J.C. All authors have read and agreed to the published version of the manuscript.

Funding: This work was supported by grants from the Canadian Institutes for Health Research PJT-1665850 (to J. Couet) and from the Fondation de l'Institut universitaire de cardiologie et de pneumologie de Québec.

Informed Consent Statement: The authors declare no conflict of interest.

Data Availability Statement: The authors will make the raw data supporting the conclusions of this article available on request.

Institutional Review Board Statement: The animal study protocol was approved by the Laval University Animal Protection Committee (protocols 2023-1549 and 2023-1550, approval February 2023).

Abbreviations

The following abbreviations are used in this manuscript:

HFpEF	Heart failure with preserved ejection fraction
AngII	Angiotensin II
MHS	Metabolic and hypertensive stress (AngII + HFD)
HFD	High-fat diet
LA	Left atrial or left atrium
LV	Left ventricle
CH	Cardiac hypertrophy
EF	Ejection fraction
UCP1	Uncoupled protein 1
ECM	Extracellular matrix
EDD	End-diastolic diameter
ESD	End-systolic diameter
RWT	Relative wall thickness
SV	Stroke volume
CO	Cardiac output
BW	Body weight
CSA	Cross-sectional area
L-NAME	L-NG-Nitroarginine Methyl Ester
BP	Blood pressure
EDV	End-diastolic volume
ESV	End-systolic volume
Nppa	Atrial natriuretic peptide
Nppb	Brain natriuretic peptide
Col1a	Pro-collagen1 alpha
Col3a	Pro-collagen3 alpha
Postn	Periostin

 doi:10.20944/preprints202509.2326.v1

Thbs4	Thrombospondin 4
PW	Posterior wall
IVSW	Interventricular septal wall
SEM	Standard error of the mean
RWT	Relative LV wall thickness
Ppia	Cyclophilin A
RPL13	L13 ribosomal protein
iNOS	Nitric oxide synthase, inducible
EF	Ejection fraction
β3-AR	Adrenergic receptor, beta 3
BAT	Brown adipose tissue
RAAS	Renin-angiotensin-aldosterone system
SNS	Sympathetic nervous system

References

1. Borlaug BA, Sharma K, Shah SJ, Ho JE. Heart Failure With Preserved Ejection Fraction: JACC Scientific Statement. J Am Coll Cardiol. 2023 May 9;81(18):1810-1834. https://doi.org/10.1016/j.jacc.2023.01.049.
2. Savarese G, Becher PM, Lund LH, Seferovic P, Rosano GMC, Coats AJS, Global burden of heart failure: a comprehensive and updated review of epidemiology, Cardiovascular Research, Volume 118, Issue 17, December 2022, Pages 3272–3287, doi.org/10.1093/cvr/cvac013.
3. Schiattarella GG, Altamirano F, Tong D, French KM, Villalobos E, Kim SY, Luo X, Jiang N, May HI, Wang ZV, Hill TM, Mammen PPA, Huang J, Lee DI, Hahn VS, Sharma K, Kass DA, Lavandero S, Gillette TG, Hill JA. Nitrosative stress drives heart failure with preserved ejection fraction. Nature. 2019 Apr;568(7752):351-356. https://doi.org/10.1038/s41586-019-1100-z.
4. Smith AN, Altara R, Amin G, Habeichi NJ, Thomas DG, Jun S, Kaplan A, Booz GW, Zouein FA. Genomic, Proteomic, and Metabolic Comparisons of Small Animal Models of Heart Failure With Preserved Ejection Fraction: A Tale of Mice, Rats, and Cats. J Am Heart Assoc. 2022 Aug 2;11(15):e026071. https://doi.org/10.1161/JAHA.122.026071.
5. Withaar C, Lam CSP, Schiattarella GG, de Boer RA, Meems LMG. Heart failure with preserved ejection fraction in humans and mice: embracing clinical complexity in mouse models. Eur Heart J. 2021 Nov 14;42(43):4420-4430. https://doi.org/10.1093/eurheartj/ehab389. Erratum in: Eur Heart J. 2022 May 21;43(20):1940. https://doi.org/10.1093/eurheartj/ehab883.
6. Jasińska-Stroschein M. Searching for Effective Treatments in HFpEF: Implications for Modeling the Disease in Rodents. Pharmaceuticals (Basel). 2023 Oct 12;16(10):1449. https://doi.org/10.3390/ph16101449.
7. Gao S, Liu XP, Li TT, Chen L, Feng YP, Wang YK, Yin YJ, Little PJ, Wu XQ, Xu SW, Jiang XD. Animal models of heart failure with preserved ejection fraction (HFpEF): from metabolic pathobiology to drug discovery. Acta Pharmacol Sin. 2024 Jan;45(1):23-35. https://doi.org/10.1038/s41401-023-01152-0.
8. Aidara ML, Walsh-Wilkinson É, Thibodeau SÈ, Labbé EA, Morin-Grandmont A, Gagnon G, Boudreau DK, Arsenault M, Bossé Y, Couët J. Cardiac reverse remodelling in a mouse model with many phenotypical features of heart failure with preserved ejection fraction: effects of modifying lifestyle. Am J Physiol Heart Circ Physiol. 2024 Apr 1;326(4):H1017-H1036. https://doi.org/10.1152/ajpheart.00462.2023.
9. Teou DC, Labbé EA, Thibodeau SÈ, Walsh-Wilkinson É, Morin-Grandmont A, Trudeau AS, Arsenault M, Couet J. The Loss of Gonadal Hormones Has a Different Impact on Aging Female and Male Mice Submitted to Heart Failure-Inducing Metabolic Hypertensive Stress. Cells. 2025 Jun 9;14(12):870. https://doi.org/10.3390/cells14120870.
10. Thibodeau SÈ, Labbé EA, Walsh-Wilkinson É, Morin-Grandmont A, Arsenault M, Couet J. Plasma and Myocardial miRNomes Similarities and Differences during Cardiac Remodelling and Reverse Remodelling in a Murine Model of Heart Failure with Preserved Ejection Fraction. Biomolecules 2024, 14, 892. https://doi.org/10.3390/biom14080892.
11. Thibodeau SÈ., Legros ML., Labbé EA, Walsh-Wilkinson É, Morin-Grandmont A, Beji S, Arsenault M, Caron A, & Couet J. (2025). Cold Exposure Exacerbates Cardiac Dysfunction in a Model of Heart Failure with Preserved Ejection Fraction in Male and Female C57Bl/6J Mice. Biomedicines 2025, 13, 1900. https://doi.org/10.3390/ biomedicines13081900.

 doi:10.20944/preprints202509.2326.v1

12. Tran HH, Thu A, Fuertes A, Gonzalez M, Twayana AR, Basta M, James M, Mahadevaiah A, Mehta KA, Islek D, Weissman S, Frishman WH, Aronow WS. Mirabegron for Cardiac Disease: A New Therapeutic Frontier. Cardiol Rev. 2025 Jun 4. https://doi.org/10.1097/CRD.0000000000000968. Epub ahead of print.
13. Michel LYM, Farah C, Balligand JL. The Beta3 Adrenergic Receptor in Healthy and Pathological Cardiovascular Tissues. Cells. 2020 Dec 2;9(12):2584. https://doi.org/10.3390/cells9122584.
14. Lin JR, Ding LL, Xu L, Huang J, Zhang ZB, Chen XH, Cheng YW, Ruan CC, Gao PJ. Brown Adipocyte ADRB3 Mediates Cardioprotection via Suppressing Exosomal iNOS. Circ Res. 2022 Jul 8;131(2):133-147. https://doi.org/10.1161/CIRCRESAHA.121.320470.
15. Zhang ZB, Cheng YW, Xu L, Li JQ, Pan X, Zhu M, Chen XH, Sun AJ, Lin JR, Gao PJ. Activation of β3-adrenergic receptor by mirabegron prevents aortic dissection/aneurysm by promoting lymphangiogenesis in perivascular adipose tissue. Cardiovasc Res. 2024 Dec 31;120(17):2307-2319. https://doi.org/10.1093/cvr/cvae213.
16. Walsh-Wilkinson É, Aidara ML, Morin-Grandmont A, Thibodeau SÈ, Gagnon J, Genest M, Arsenault M, Couet J. Age and sex hormones modulate left ventricle regional response to angiotensin II in male and female mice. Am J Physiol Heart Circ Physiol. 2022 Oct 1;323(4):H643-H658. https://doi.org/10.1152/ajpheart.00044.2022.
17. Labbé EA, Thibodeau SÈ, Walsh-Wilkinson É, Chalifour M, Sirois PO, Leblanc J, Morin-Grandmont A, Arsenault M, Couet J. Relative contribution of correcting the diet and voluntary exercise to myocardial recovery in a two-hit murine model of heart failure with preserved ejection fraction. Am J Physiol Heart Circ Physiol. 2025 Jul 1;329(1):H51-H68. https://doi.org/10.1152/ajpheart.00092.2025.
18. Le Lay S, Scherer PE. Exploring adipose tissue-derived extracellular vesicles in inter-organ crosstalk: Implications for metabolic regulation and adipose tissue function. Cell Rep. 2025 Jun 24;44(6):115732. https://doi.org/10.1016/j.celrep.2025.115732.
19. Zhao S, Kusminski CM, Scherer PE. Adiponectin, Leptin and Cardiovascular Disorders. Circ Res. 2021 Jan 8;128(1):136-149. https://doi.org/10.1161/CIRCRESAHA.120.314458.
20. McLeod K, Datta V, Fuller S. Adipokines as Cardioprotective Factors: BAT Steps Up to the Plate. Biomedicines. 2025 Mar 13;13(3):710. https://doi.org/10.3390/biomedicines13030710.
21. Villarroya F, Cereijo R, Villarroya J, Giralt M. Brown adipose tissue as a secretory organ. Nat Rev Endocrinol. 2017 Jan;13(1):26-35. https://doi.org/10.1038/nrendo.2016.136.
22. Finlin BS, Memetimin H, Confides AL, Kasza I, Zhu B, Vekaria HJ, Harfmann B, Jones KA, Johnson ZR, Westgate PM, Alexander CM, Sullivan PG, Dupont-Versteegden EE, Kern PA. Human adipose beiging in response to cold and mirabegron. JCI Insight. 2018 Aug 9;3(15):e121510. https://doi.org/10.1172/jci.insight.121510.
23. Bel JS, Tai TC, Khaper N, Lees SJ. Mirabegron: The most promising adipose tissue beiging agent. Physiol Rep. 2021 Mar;9(5):e14779. https://doi.org/10.14814/phy2.14779.
24. Altınova AE. Beige Adipocyte as the Flame of White Adipose Tissue: Regulation of Browning and Impact of Obesity. J Clin Endocrinol Metab. 2022 Apr 19;107(5):e1778-e1788. https://doi.org/10.1210/clinem/dgab921.
25. Cheng HJ, Zhang ZS, Onishi K, Ukai T, Sane DC, Cheng CP. Upregulation of functional beta(3)-adrenergic receptor in the failing canine myocardium. Circ Res. 2001 Sep 28;89(7):599-606. https://doi.org/10.1161/hh1901.098042.
26. Moniotte S, Kobzik L, Feron O, Trochu JN, Gauthier C, Balligand JL. Upregulation of beta(3)-adrenoceptors and altered contractile response to inotropic amines in human failing myocardium. Circulation. 2001 Mar 27;103(12):1649-55. https://doi.org/10.1161/01.cir.103.12.1649.
27. Treskatsch S, Feldheiser A, Rosin AT, Sifringer M, Habazettl H, Mousa SA, Shakibaei M, Schäfer M, Spies CD. A modified approach to induce predictable congestive heart failure by volume overload in rats. PLoS One. 2014 Jan 31;9(1):e87531. https://doi.org/10.1371/journal.pone.0087531.
28. Gauthier C, Leblais V, Kobzik L, Trochu JN, Khandoudi N, Bril A, Balligand JL, Le Marec H. The negative inotropic effect of beta3-adrenoceptor stimulation is mediated by activation of a nitric oxide synthase pathway in human ventricle. J Clin Invest. 1998 Oct 1;102(7):1377-84. https://doi.org/10.1172/JCI2191.

29. Nerea Hermida, Lauriane Michel, Hrag Esfahani, Emilie Dubois-Deruy, Joanna Hammond, Caroline Bouzin, Andreas Markl, Henri Colin, Anne Van Steenbergen, Christophe De Meester, Christophe Beauloye, Sandrine Horman, Xiaoke Yin, Manuel Mayr, Jean-Luc Balligand, Cardiac myocyte β3-adrenergic receptors prevent myocardial fibrosis by modulating oxidant stress-dependent paracrine signaling, European Heart Journal, Volume 39, Issue 10, 07 March 2018, Pages 888–898. https://doi.org/10.1093/eurheartj/ehx366.
30. Michel LYM, Esfahani H, De Mulder D, Verdoy R, Ambroise J, Roelants V, Bouchard B, Fabian N, Savary J, Dewulf JP, Doumont T, Bouzin C, Haufroid V, Luiken JJFP, Nabben M, Singleton ML, Bertrand L, Ruiz M, Des Rosiers C, Balligand JL. An NRF2/β3-Adrenoreceptor Axis Drives a Sustained Antioxidant and Metabolic Rewiring Through the Pentose-Phosphate Pathway to Alleviate Cardiac Stress. Circulation. 2025 May 6;151(18):1312-1328. https://doi.org/10.1161/CIRCULATIONAHA.124.067876.
31. Andersson KE, Martin N, Nitti V. Selective β_3-adrenoceptor agonists for the treatment of overactive bladder. J Urol. 2013 Oct;190(4):1173-80. https://doi.org/10.1016/j.juro.2013.02.104.
32. Balligand JL, Brito D, Brosteanu O, Casadei B, Depoix C, Edelmann F, Ferreira V, Filippatos G, Gerber B, Gruson D, Hasenclever D, Hellenkamp K, Ikonomidis I, Krakowiak B, Lhommel R, Mahmod M, Neubauer S, Persu A, Piechnik S, Pieske B, Pieske-Kraigher E, Pinto F, Ponikowski P, Senni M, Trochu JN, Van Overstraeten N, Wachter R, Pouleur AC. Repurposing the β3-Adrenergic Receptor Agonist Mirabegron in Patients With Structural Cardiac Disease: The Beta3-LVH Phase 2b Randomized Clinical Trial. JAMA Cardiol. 2023 Nov 1;8(11):1031-1040. https://doi.org/10.1001/jamacardio.2023.3003.
33. Bundgaard H, Axelsson Raja A, Iversen K, Valeur N, Tønder N, Schou M, Christensen AH, Bruun NE, Søholm H, Ghanizada M, Fry NAS, Hamilton EJ, Boesgaard S, Møller MB, Wolsk E, Rossing K, Køber L, Rasmussen HH, Vissing CR. Hemodynamic Effects of Cyclic Guanosine Monophosphate-Dependent Signaling Through β3 Adrenoceptor Stimulation in Patients With Advanced Heart Failure: A Randomized Invasive Clinical Trial. Circ Heart Fail. 2022 Jul;15(7):e009120. https://doi.org/10.1161/CIRCHEARTFAILURE.121.009120.
34. Bahrami HSZ, Hasselbalch RB, Søholm H, Thomsen JH, Sørgaard M, Kofoed KF, Valeur N, Boesgaard S, Fry NAS, Møller JE, Raja AA, Køber L, Iversen K, Rasmussen H, Bundgaard H. First-In-Man Trial of β3-Adrenoceptor Agonist Treatment in Chronic Heart Failure: Impact on Diastolic Function. J Cardiovasc Pharmacol. 2024 May 1;83(5):466-473. https://doi.org/10.1097/FJC.0000000000001545. PMID: 38452283.
35. García-Álvarez A, Blanco I, García-Lunar I, Jordà P, Rodriguez-Arias JJ, Fernández-Friera L, Zegri I, Nuche J, Gomez-Bueno M, Prat S, Pujadas S, Sole-Gonzalez E, Garcia-Cossio MD, Rivas M, Torrecilla E, Pereda D, Sanchez J, García-Pavía P, Segovia-Cubero J, Delgado JF, Mirabet S, Fuster V, Barberá JA, Ibañez B; SPHERE-HF Investigators. β3 adrenergic agonist treatment in chronic pulmonary hypertension associated with heart failure (SPHERE-HF): a double blind, placebo-controlled, randomized clinical trial. Eur J Heart Fail. 2023 Mar;25(3):373-385. https://doi.org/10.1002/ejhf.2745.
36. Poekes L, Gillard J, Farrell GC, Horsmans Y, Leclercq IA. Activation of brown adipose tissue enhances the efficacy of caloric restriction for treatment of nonalcoholic steatohepatitis. Lab Invest. 2019 Jan;99(1):4-16. https://doi.org/10.1038/s41374-018-0120-x.
37. Sui W, Li H, Yang Y, Jing X, Xue F, Cheng J, Dong M, Zhang M, Pan H, Chen Y, Zhang Y, Zhou Q, Shi W, Wang X, Zhang H, Zhang C, Zhang Y, Cao Y. Bladder drug mirabegron exacerbates atherosclerosis through activation of brown fat-mediated lipolysis. Proc Natl Acad Sci U S A. 2019 May 28;116(22):10937-10942. https://doi.org/10.1073/pnas.1901655116.
38. Peres Valgas da Silva C, Calmasini F, Alexandre EC, Raposo HF, Delbin MA, Monica FZ, Zanesco A. The effects of mirabegron on obesity-induced inflammation and insulin resistance are associated with brown adipose tissue activation but not beiging in the subcutaneous white adipose tissue. Clin Exp Pharmacol Physiol. 2021 Nov;48(11):1477-1487. https://doi.org/10.1111/1440-1681.13566.
39. Komatsu Y, Aoyama K, Yoneda M, Ito S, Sano Y, Kawai Y, Cui X, Yamada Y, Furukawa N, Ikeda K, Nagata K. Surgical ablation of whitened interscapular brown fat ameliorates cardiac pathology in salt-loaded metabolic syndrome rats. Ann N Y Acad Sci. 2021 May;1492(1):11-26. https://doi.org/10.1111/nyas.14546.
40. Jiang P, Cheng B, Wang Z, Zheng Z, Duan Q. Distinct effects of physical and functional ablation of brown adipose tissue on T3-dependent pathological cardiac remodeling. Biochem Biophys Res Commun. 2024 Nov 26;735:150844. https://doi.org/10.1016/j.bbrc.2024.150844.

 doi:10.20944/preprints202509.2326.v1

41. Zhao H, Chen X, Hu G, Li C, Guo L, Zhang L, Sun F, Xia Y, Yan W, Cui Z, Guo Y, Guo X, Huang C, Fan M, Wang S, Zhang F, Tao L. Small Extracellular Vesicles From Brown Adipose Tissue Mediate Exercise Cardioprotection. Circ Res. 2022 May 13;130(10):1490-1506. https://doi.org/10.1161/CIRCRESAHA.121.320458.
42. Ruan CC, Kong LR, Chen XH, Ma Y, Pan XX, Zhang ZB, Gao PJ. A_{2A} Receptor Activation Attenuates Hypertensive Cardiac Remodeling via Promoting Brown Adipose Tissue-Derived FGF21. Cell Metab. 2018 Sep 4;28(3):476-489.e5. https://doi.org/10.1016/j.cmet.2018.06.013. Epub 2018 Jul 12. Erratum in: Cell Metab. 2020 Oct 6;32(4):689. https://doi.org/10.1016/j.cmet.2020.08.018.
43. Ding Y, Su J, Shan B, Fu X, Zheng G, Wang J, Wu L, Wang F, Chai X, Sun H, Zhang J. Brown adipose tissue-derived FGF21 mediates the cardioprotection of dexmedetomidine in myocardial ischemia/reperfusion injury. Sci Rep. 2024 Aug 7;14(1):18292. https://doi.org/10.1038/s41598-024-69356-w.
44. McLeod K, Datta V, Fuller S. Adipokines as Cardioprotective Factors: BAT Steps Up to the Plate. Biomedicines. 2025 Mar 13;13(3):710. https://doi.org/10.3390/biomedicines13030710. PMID: 40149686; PMCID: PMC11940801.
45. Zhang ZB, Cheng YW, Xu L, Li JQ, Pan X, Zhu M, Chen XH, Sun AJ, Lin JR, Gao PJ. Activation of β3-adrenergic receptor by mirabegron prevents aortic dissection/aneurysm by promoting lymphangiogenesis in perivascular adipose tissue. Cardiovasc Res. 2024 Dec 31;120(17):2307-2319. https://doi.org/10.1093/cvr/cvae213.
46. Challa AA, Vidal P, Maurya SK, Maurya CK, Baer LA, Wang Y, James NM, Pardeshi PJ, Fasano M, Carley AN, Stanford KI, Lewandowski ED. UCP1-dependent brown adipose activation accelerates cardiac metabolic remodeling and reduces initial hypertrophic and fibrotic responses to pathological stress. FASEB J. 2024 Jun 15;38(11):e23709. https://doi.org/10.1096/fj.202400922R.
47. Nag, S.; Patel, S.; Mani, S.; Hussain, T. Role of angiotensin type 2 receptor in improving lipid metabolism and preventing adiposity. *Mol. Cell. Biochem.* **2019**, *461*, 195–204. https://doi.org/10.1007/s11010-019-03602-y.
48. Nag, S.; Khan, M.A.; Samuel, P.; Ali, Q.; Hussain, T. Chronic angiotensin AT2R activation prevents high-fat diet-induced adiposity and obesity in female mice independent of estrogen. *Metabolism* **2015**, *64*, 814–825. https://doi.org/10.1016/j.metabol.2015.01.019.
49. Than, A.; Xu, S.; Li, R.; Leow, M.-S.; Sun, L.; Chen, P. Angiotensin type 2 receptor activation promotes browning of white adipose tissue and brown adipogenesis. Signal Transduct. *Target. Ther.* **2017**, *2*, 17022. https://doi.org/10.1038/sigtrans.2017.22.
50. Zhao XY, Liu Y, Zhang X, Zhao BC, Burley G, Yang ZC, Luo Y, Li AQ, Zhang RX, Liu ZY, Shi YC, Wang QP. The combined effect of metformin and mirabegron on diet-induced obesity. MedComm (2020). 2023 Feb 14;4(2):e207. https://doi.org/10.1002/mco2.207.